Response of Plastic Shells with Metal Cores to Transient External Pressures

G. S. SAMUELSEN*
University of California, Irvine, Calif.

AND

WILLEM STUIVER†
University of Hawaii, Honolulu, Hawaii

An analysis of the response of plastic shells with solid metal cores to transient external pressures is presented. Failure criteria are determined for shells exposed to pressure pulses with a step rise and an exponential decay. Modes of failure considered are cracking and spalling. Conditions of failure are calculated for linear-elastic shell materials by means of both graphical and numerical methods, the graphical method providing a more descriptive picture of the stress-wave motion following incidence of the pulse. The graphical results show that pulses of the type considered may be classified in three groups (pulses with fast, moderate, and slow decay) depending on the response mechanism produced. The numerical method is more powerful since it allows the consideration of particle velocity effects, and of nonelastic as well as nonlinear material properties in addition to the linear-elastic analysis. Nonlinear effects are found to be more important than nonelastic effects. For pulses of long duration, the numerical results show that the effect of particle velocity cannot be neglected; for impulsive loads (short pulse duration), the numerical results show that the graphical method is adequate.

1. Introduction

IN Fig. 1a, a cross section of a cylindrical plastic shell with a metal core is shown. If a uniform external pressure is suddenly applied to the outer surface of the shell, a shock wave will propagate into the shell from the loaded surface. When the shock arrives at the shell-core interface, a shock will be transmitted into the core and, because metals generally have higher shock impedances than plastics, a shock will also be reflected back into the shell. The reflected shock travels back to the loading surface where it is reflected as rarefaction (tension) wave. If the load has decayed prior to the arrival of the reflected shock at the loading surface, the rarefaction wave will produce radial tensile stresses in the shell. If the radial tensile stresses are sufficiently great, spalling of the plastic will occur. An example of spalling is shown in Fig. 1b.

If the radial tensile stresses in the reflected wave are insufficient to spall the shell, the wave will propagate to the shell-core interface and, assuming negligible tensile strength of the bond at the interface, the shell will separate from the core. If the outward velocity of the shell is sufficiently great, the shell will develop tensile hoop stresses intense enough to produce fractures. This response is called rebound cracking, an example of which is shown in Fig. 1c. Spalling and rebound cracking can also occur together. The shell first spalls and, as a result of separation, develops hoop stresses that produce cracking.

In the present study critical loads for producing spalling and rebound cracking are determined for surface pressures with a step rise and an exponential decay. Because these loads depend on the intensity of the incident pulse, it is found convenient to plot critical load boundaries (failure boundaries) in planes defined by parameters that characterize the pulse. For loads with a steep rise and gradual decay, such parameters are the peak pressure P_0 and the total impulse I. These two parameters are identified in Fig. 2 for the exponential pulse considered here.

Received December 4, 1970; revision received May 4, 1971. This work was conducted at Stanford Research Institute, Menlo Park, Calif., and supported by the Air Force Special Weapons Center under Contract AF29(601)-6828. The authors gratefully acknowledge the helpful discussions and suggestions of the principal investigator on the project, G. R. Abrahamson.

* Assistant Professor, School of Engineering.

† Professor and Chairman, Department of Mechanical Engineering.

2. Approach

There are three basic methods available for studying stress-wave behavior: analytical, graphical, and numerical. The analytical and graphical methods have been successful where the peak pressure of the pulse is sufficiently low to utilize linear wave theory. The analytical method can become tedious, however. In addition, analytical solutions are not easily obtained for all conditions. The graphical solution is not so confined. Solutions can be obtained for most conditions and the graphical method provides a greater insight into the stress-wave action that produces spalling and cracking.

Under high pressures materials may exhibit nonlinear or nonelastic properties or both, and the use of analytical and graphical methods may not be justified. In cases where the peak pressures are high, a numerical method may be required.

In the present study, the critical loads for spalling and cracking of a plastic shell on a metal base are determined using the graphical and numerical methods and the results compared. The plastic shell is taken to be thin compared to its radius, consistent with many cases of practical interest. For such a geometry the stress waves can be regarded as one-dimensional, propagating in the radial direction only. The bond strength between the plastic shell and the base is assumed to be zero.

3. Graphical Method

The linear-elastic problem of stress wave propagation in a two-layered laminate has been studied previously by means of a simple graphical procedure for uniform[1] and matched pulses.[2,3] The basic parameters governing the process of

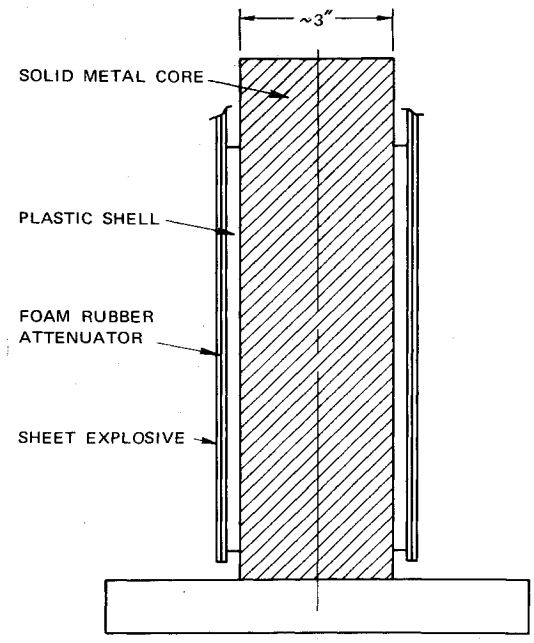

Fig. 1a Experiment demonstrating response of plastic shell on solid base.

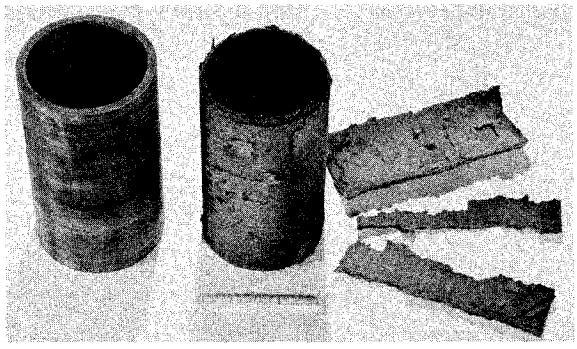

Fig. 1b Failure of plastic shell by spalling.

Fig. 1c Failure of plastic shell by rebound cracking.

stress wave propagation are K and e.[2,3,4] The reflection coefficient K is defined as

$$K = [1 - (\rho c/\rho_b c_b)]/[1 + (\rho c)/(\rho_b c_b)] \quad (1)$$

where ρc is the acoustic impedance and the subscript b refers to the base. The parameter e is a measure of the pressure decay in the pulse and is defined as

$$e = \exp(-\lambda\gamma) \quad (2)$$

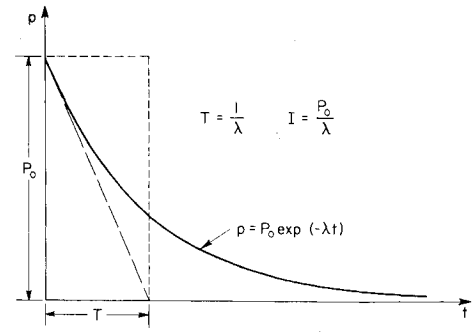

Fig. 2 Exponential pulse.

where $\lambda = 1/T$ and γ is twice the transit time of the shell.

An incident pulse with a step-rise and exponential decay may be conveniently divided into three significant groups: pulses with slow, moderate and fast decay.[4] The distinction between the three groups is based on the parameters K and e as shown in Fig. 3.

Exponential pulses with slow decay: For the case $K \leq e$ tensile stresses do not develop in the shell and failure by spalling cannot occur. In addition, pressure is maintained at the interface between the shell and base preventing separation and any subsequent failure by cracking.

Exponential pulses with fast decay: The class of exponential pulses with fast decay is characterized by the condition $e \leq K/(K + 1)$. For this class of pulses the decay of pressure is sufficiently fast to promote separation of the shield from the base at the instant of the second peak reflection from the interface. The shell remains separated from the base for all subsequent time and recombination does not take place.

Exponential pulses with moderate decay: This case is more complicated because separation of the shell and base is followed by recombination. Depending upon the magnitude of the residual load at separation, such recombination may occur repeatedly. Exponential pulses with moderate decay are characterized by the condition, $K/(K + 1) < e < K$.

Failure criteria: Cracking of the shell is taken to occur if the circumferential tensile stress generated during separation exceeds a critical value σ_{cr}; spalling is taken to occur if radial stresses generated in the shell exceed a critical value σ_{sp}. Since the problem is taken to be linear in the graphical approach, stresses generated are proportional to the peak pressure P_0 of the incident pulse. Thus, for the circumferential

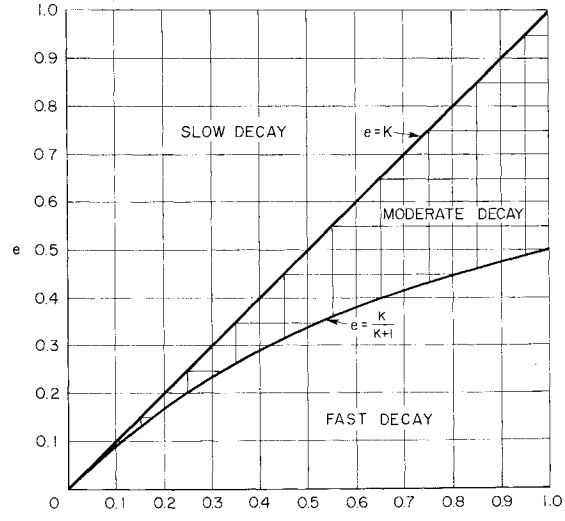

Fig. 3 Slow, moderate, and fast decay regions in K,e plane.

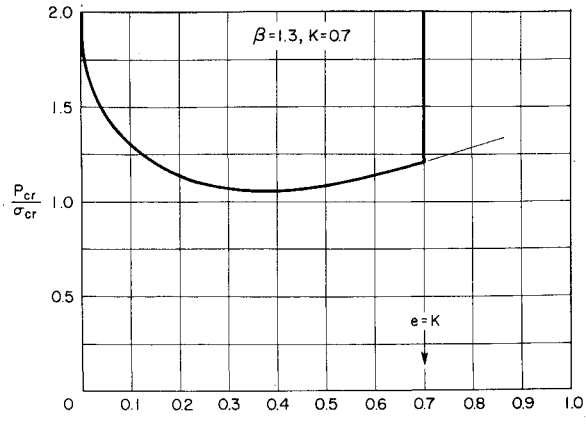

Fig. 4 Cracking boundary for exponential pulses in terms of e.

and radial stresses σ_0 and σ_r, respectively, we may write

$$\sigma_0 = P_0 C(a_i), \quad \sigma_r = P_0 S(a_i) \tag{3}$$

where C and S depend through the parameters a_i on the shape of the pulse and the properties of the laminate. Then, for cracking we must have

$$P_0 \geq P_{cr} = \sigma_{cr}/C(a_i) \tag{4}$$

and, for spalling

$$P_0 \leq P_{sp} = \sigma_{sp}/S(a_i) \tag{5}$$

These relations define failure boundaries once the functions C and S are known.

Failure Boundaries

Cracking: To determine the cracking boundary we regard the shell upon separation as a ring in uniform radial motion. Cracking occurs if the outward displacement becomes sufficiently large to generate tensile stresses in the shell that exceed the fracture limit. For pulses with slow decay ($K \leq e$) separation does not occur; hence, cracking is not possible. For pulses with moderate or fast decay ($K > e$) separation always occurs; cracking is then possible if the peak pressure of the incident pulse is sufficiently high.

To determine the maximum outward displacement of the shell, the average outward velocity at the instant of separation is required. For pulses with fast decay, permanent separation of shell and base occurs at the instant $t = 1.5\gamma$. For pulses with moderate decay, the average outward velocity of the shell is greatest at first separation[4] (at $t = 1.5\gamma$). Hence, the average velocity needed to determine the maximum outward displacement is the one at $t = 1.5\gamma$ for all pulses.

An expression for this velocity in terms of the basic parameters K and e can be found for all cases.[4] The maximum outward displacement of the shell is determined directly from the average initial outward velocity by equating corresponding potential and kinetic energies.‡ The resulting expression for the function C in Eq. (4) is

$$C = 1/2\beta[K - (1 - K)e + (2K - e)e^{1/2}] \tag{6}$$

where

$$\beta = c_r/c_\theta = [(1 - \nu)^2/(1 - 2\nu)]^{1/2}$$

The corresponding cracking boundary is shown in Fig. 4 for the properties of Table 1 ($\beta = 1.3$, $K = 0.7$). Transformation of this boundary to the pressure-impulse plane of Fig. 5 involves the relations $\ln e = -\lambda\gamma$, $I_{cr} = P_{cr}/\lambda$, and the definition $I_{cr} = I^*\sigma_{cr}\gamma/2$; that is

$$I^* = 2P_{cr}/[\sigma_{cr} \ln(1/e)] \tag{7}$$

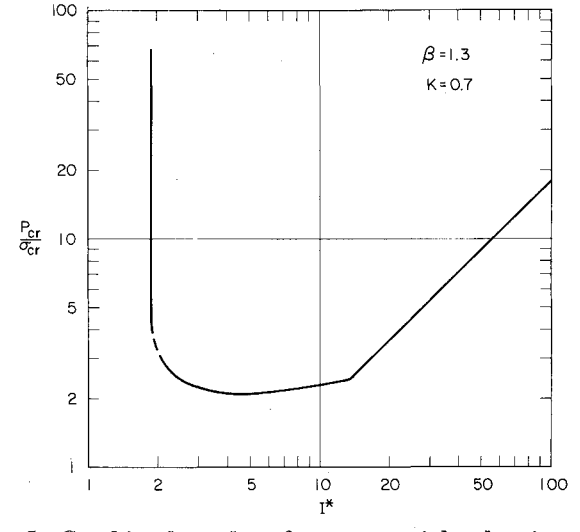

Fig. 5 Cracking boundary for exponential pulses in pressure-impulse plane.

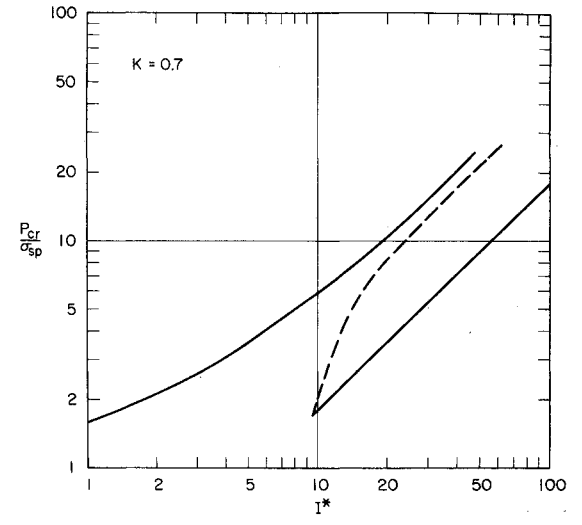

Fig. 6 Spall boundary for exponential pulses.

Spalling: For pulses with slow decay ($K \leq e$), radial tensile stresses do not occur; hence, spall is not possible. For pulses with moderate or fast decay ($K > e$), radial tensile stresses always occur, and spall is possible if the peak pressure of the incident pulse is sufficiently high. For pulses with fast decay, the function S in Eq. (5) assumes the form[4]

$$S = K - (1 + K)e \tag{8}$$

A corresponding expression for pulses with moderate decay is less easily established. Different expressions apply depending upon the value of e in terms of K. Calculations, given in Ref. 4, show that approximate expressions for S can be found in the various regions. The resulting spall boundary is given in Fig. 6 (the dashed part of the boundary curve indicates an approximation).

4. Numerical Method

In the previous section, the response of a plastic shell on a thick base was analyzed for linear-elastic materials using graphical methods. Under high pressures, some materials

‡ This assumes that the effect of incident pressures acting after the instant of separation is negligible, an assumption not always valid. The effect of incident pressures acting after separation is considered for in Sec. 5.

Table 1 Material properties

Material	Density, g/cm³, ρ_0	Sound speed, cm/μsec, c_0	Acoustic impedance, barsec/cm, $\rho_0 c_0$	Yield stress, *kbar*, σ_{cr}	Poisson's ratio, ν	Thickness, cm, h	Mean radius, cm, r_m
Epoxy shell	1.18	0.265	0.313	3.0	0.4	2.54	38.1
Aluminum base (6061-T6)	2.79	0.640	1.761	5.0	0.3	"Infinite"	...

exhibit strong nonlinear properties and may respond plastically. Such conditions introduce complex interactions between variables to which the graphical method cannot be applied. Only numerical techniques have been successful in obtaining solutions to the wave equations for such cases.

The primary purpose of this section is to determine critical load boundaries for rebound cracking of the shell taking into account nonlinear and plastic effects on stress-wave propagation.

In the present study a computer code was modified to study the effect of nonlinear properties and plastic response on the failure modes. The calculations are divided into two parts: 1) *"early-time" stress wave propagation* in the composite prior to separation, and 2) *"late-time" structural displacement* of the shell after separation. The early-time stress-wave calculations yield the rebound velocity of the shell; this velocity then serves as the initial condition for the late-time structural displacement calculations.

The early-time stress-wave calculations are made using the Q-method of von Neumann and Richtmyer.[5] The code used here is based on numerical techniques developed by White and Griffis,[6] Wood,[7] and Morland,[8] and generalized by Erkman.[9] The late-time structural displacement model used is a ring in uniform radial motion, regarded as a linear oscillator. The maximum displacement is found for the velocity at separation and the incident load acting after separation. Cracking is taken to occur if the displacement exceeds a critical value.

The material properties are described in Table 1. The shell and base were epoxy and aluminum and the shell thickness was arbitrarily chosen to be 2.54 cm.

Early-Time Stress-Wave Calculations

The equations of continuity and motion for one-dimensional flow in Lagrangean coordinates are[3]

$$\rho_0 \partial V/\partial t = \partial u/\partial x \tag{9}$$

$$\rho_0 \partial u/\partial t = -\partial(p_x + Q)/\partial x \tag{10}$$

where u is particle velocity, $V = 1/\rho$, ρ_0 is the initial density, and Q is the artificial viscosity parameter. Q is taken here to be

$$Q = -(1/V)(\partial u/\partial x)(|\partial u/\partial x| i^2 + nc) \tag{11}$$

where $i = 1.7$, $n = 0.2$, and c is the local sound speed.

The shell and base materials are represented by the elastoplastic model of Fig. 7. With this model, the material behaves elastically along ba, where a is the yield point in compression. Segment ae is the locus of plastic loading states, ef the locus of elastic unloading states, and fb the locus of plastic unloading states. In one-dimensional compression, the mean pressure and maximum resolved shear stress are

$$d\bar{p} = \tfrac{1}{3} d(p_x + p_y + p_z) \tag{12}$$

$$d\tau = (dp_x - dp_y)/2 \tag{13}$$

and the compressive stress in the direction of propagation is given by

$$dp_x = d\bar{p} + \tfrac{4}{3} d\tau \tag{14}$$

$\bar{p}(\rho)$ can be expressed conveniently as[10]

$$\bar{p} = A\mu + B\mu^2 + C\mu^3 \tag{15}$$

where $\mu = \rho/\rho_0 - 1$ and A, B, and C are constants depending on the material (see Fig. 7).

For the numerical calculations, Eq. (9) and (10) were written in difference form, programed in ALGOL, and numerically integrated for the given initial conditions using the relations of Fig. 7 (Ref. 4).

The output of the early time stress-wave calculations includes 1) the occurrence and time of spall, 2) the time of separation, and 3) the rebound velocity and displacement of the shell at separation. The latter become the initial velocity and displacement for the late-time structural displacement calculations.

Late-Time Structural Displacement Calculations

For the displacement of the shell after separation, the structural model is taken as a ring behaving as a linear oscillator. The equation of motion for a linear oscillator (neglecting damping and using $r \equiv x$) is

$$\ddot{r} + (k/m)r = F(t)/m \tag{16}$$

where r is the radial displacement from the mean radius r_m before separation, m is the mass per unit circumferential length, $F(t)$ the forcing function, and k the spring constant. In the present problem, Eq. (16) is readily solved in terms of r for the exponential pulse of Fig. 2 and the material properties of Table 1 (Ref. 4).

Failure Criteria

The criteria for cracking may be simplified for pulses that do not act after separation. Hence, it is convenient to consider separately the failure criteria for pulses which act after separation and those that do not. These pulses are referred to here as long and short pulses, respectively.

Cracking—long pulses: A critical displacement of the shell for which cracking occurs may be calculated based on

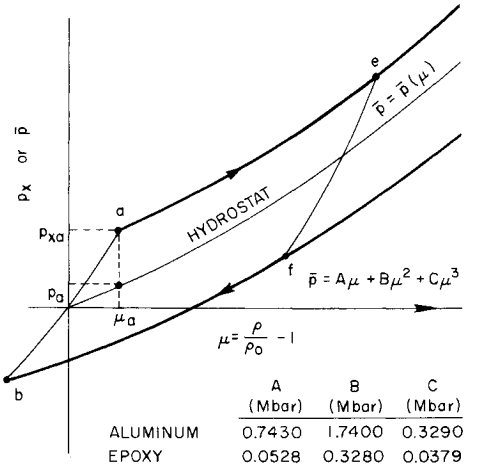

Fig. 7 Elastoplastic cycle.

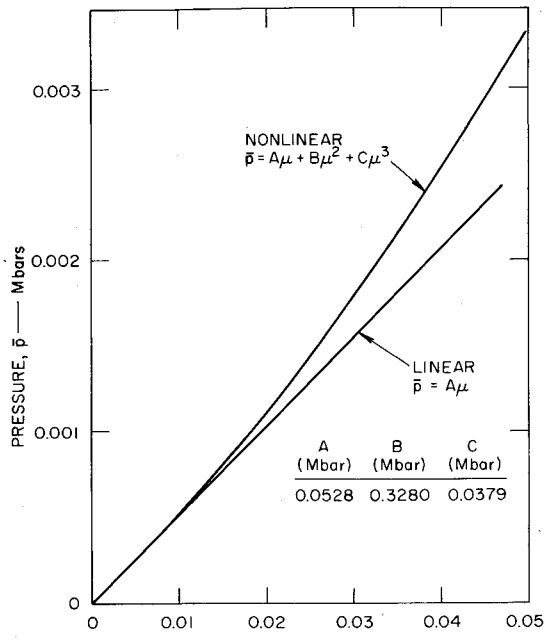

Fig. 8 Comparison of nonlinear and linear equations of state for epoxy.

Hooke's law as follows:

$$(r - r_m)/r_m = \sigma_\theta E_\theta \tag{17}$$

Using $E_\theta = \rho c_\theta^2$ and putting $\Delta r_{cr} = (r_{cr} - r_m)$ and $\sigma_\theta = \sigma_{\theta cr}$, Eq. (17) becomes

$$\Delta r_{cr} = \sigma_{\theta cr}(\beta^2/\rho c_r) r_m \tag{18}$$

where β is defined by Eq. (6). For the properties of Table 1, the critical displacement for the epoxy shell is $\Delta r_{cr} = 2.48$ cm. For pulses which act after separation (long pulses), the solution to Eq. (16) is used to determine the maximum outward displacement of the shell based on the velocity at separation and load action after separation. Should the maximum displacement be in excess of the critical displacement of 2.48 cm, cracking is assumed to occur.

Cracking—short pulses: If the incident pulse does not act beyond separation (short pulses), the late-time structural displacement calculation is not necessary. Instead a critical separation velocity sufficient to project the shell to or beyond the point of the critical displacement (2.48 cm) may be defined. If the velocity at separation is greater than the critical value then cracking occurs.

If v_s is the velocity at separation, the kinetic energy (per unit area) is

$$KE = \tfrac{1}{2}\rho h(v_s)^2 \tag{19}$$

For uniform radial displacement, the strain energy is

$$SE = \frac{1}{2}\frac{h}{E_\theta}\sigma_\theta^2 \tag{20}$$

For the critical condition, σ_θ becomes the maximum hoop stress $\sigma_{\theta cr}$. Equating the strain energy to the kinetic energy at separation and solving for $v_s = v_{cr}$, the critical separation velocity becomes

$$v_{cr} = \sigma_{\theta cr}/(E_\theta \rho)^{1/2} = B\sigma_{\theta cr}/\rho c \tag{21}$$

Taking $\sigma_{\theta cr} = 3$ kbar and the properties of Table 1

$$v_{cr} = 12.88 \text{ cm/ms}$$

Spalling: Spall failure was assumed to occur in the epoxy shell if the tensile stress exceeded the yield stress of the epoxy, 3.0 kbar.

Failure Boundaries

Critical load boundaries for rebound cracking of the shell were generated for an exponential pulse applied to an epoxy shell and aluminum base described by the model of Fig. 7.

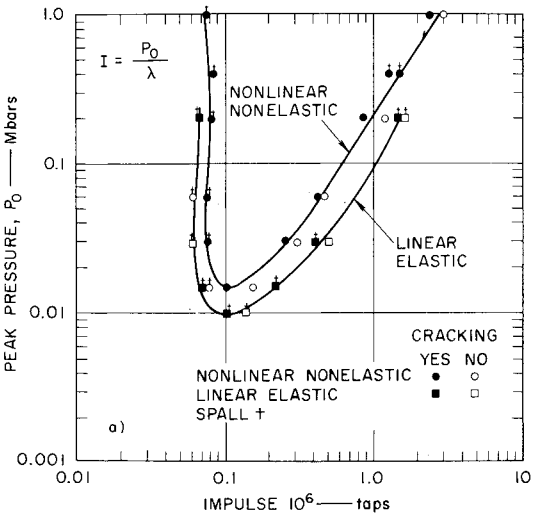

a) Nonlinear-nonelastic, linear-elastic

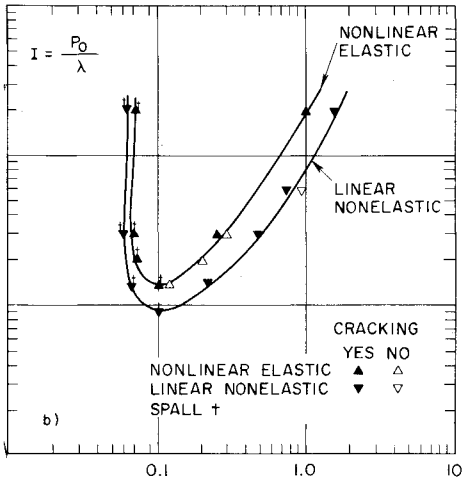

b) Nonlinear-elastic, linear-nonelastic

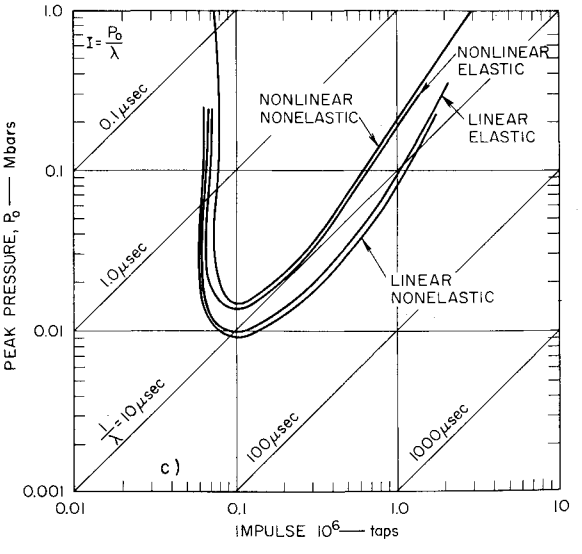

c) a and b combined

Fig. 9 Cracking boundaries for exponential pulses.

Effects of differences in material properties were examined for the following cases: 1) nonlinear-nonelastic (A, B, C, $\neq 0$ in Eq. (15)); 2) nonlinear-elastic ($p_{xa} = \infty$ in Fig. 7); 3) linear-elastic (B, $C = 0$; $p_{xa} = \infty$); 4) linear-nonelastic ($B = C = 0$). The differences between the nonlinear and linear constitutive relations can be seen in Fig. 8.

Figures 9a and 9b show the results of the computer runs and the cracking boundaries determined from them. As expected, the boundaries all exhibit a minimum, are impulse-dependent for low impulses, and rise monotonically beyond the minimum. Spall occurred as shown.

Effects of differences in constitutive relations of shell and base: Effects of differences in the constitutive relations of the shell and base are combined in Fig. 9c (obtained from 9a and b). For the range of differences considered here, nonlinear effects are much more significant than plasticity effects.

Nonlinear effects result in a difference of about 40% in critical pressure at the minimum. To the right of the minimum, nonlinear effects produce differences of about 40% or less in both pressure and impulse. To the left of the minimum (in the region where the curves rise rapidly) only the impulse is significant and differences in impulse due to nonlinear effects are about 15%. In contrast to the nonlinear effects, plasticity effects result in differences of less than 10% everywhere.

Nonlinearities affect the critical load curves primarily through increases in shock velocity with pressure, which result in earlier separation for the nonlinear material. This decreases the rebound velocity and, due to the higher load remaining at the earlier separation, causes the shell to experience more rapid deceleration after separation. Thus, the load amplitude required to develop a given displacement is higher for the nonlinear material.

5. Summary

The graphical results indicate that the exponential pulse can be divided into three important groups: slow, fast, and moderate decay. These groups are distinguished by the parameters K and e. The regions corresponding to each pulse are identified in Fig. 3. For pulses with slow decay separation of shell and base does not occur nor do tensile stresses. Hence, the danger of cracking or spalling does not exist. For pulses with fast or moderate decay, separation always takes place. Cracking and/or spalling is then possible if the peak pressure is sufficiently high. Separation is permanent (in the plane model) for pulses with fast decay; the problem of failure is then easily solved. For pulses with moderate decay, separation of shell and base is followed by recombination which may occur repeatedly; the problem of failure becomes then much more involved.

Figure 10 summarizes the cracking boundaries calculated for pulses with a step rise and an exponential decay for both

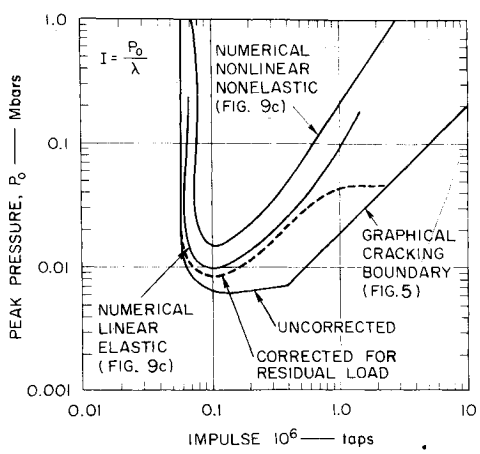

Fig. 10 Cracking boundary for exponential pulses.

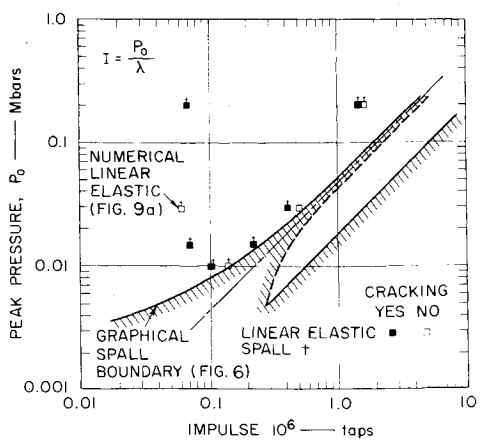

Fig. 11 Spall boundary for exponential pulses.

the graphical and numerical methods. The two upper curves are from the numerical analysis and are the same as those of Fig. 9. The lower curve is from the graphical analysis and is obtained from Fig. 5, using the material properties and dimensions from Table 1.

The failure boundary from the graphical analysis lies below the boundary from the numerical analysis, with the difference becoming greater at high impulses. The difference is attributed to the effects of the load acting after separation and to the contribution of particle velocity to the wave propagation velocity, which are accounted for in the numerical analysis but not in the graphical analysis. Both of these effects would be expected to raise the failure boundary and would be greater at larger impulses (longer pulse duration).

The load acting after separation (residual load) may be numerically calculated as a late-time structural displacement addendum to the graphical analysis just as it is in the numerical analysis. If this is done, the dotted ("corrected") curve in Fig. 10 is obtained and the effect of the residual load is found to be important. It is also seen by the departure of the numerical and graphical boundaries that the contribution of particle velocity becomes significant for high values of impulses.

Figure 11 shows the graphical spall boundary for exponential pulses. The spall region to the right of the dashed line of unit slope is due to the effect of recombination at the shell-base interface. The results of the numerical calculations are given by the points, the crosses indicating spalling. The distribution of the points, which was chosen to determine the cracking boundary, is not ideal for comparison with the graphical spall boundary. However, the points that are available agree well. The most significant agreement is near the center of the middle square, where spall and no-spall points come close to bracketing the graphical boundary. The difference is attributed to the effect of particle velocity on wave velocity.

The foregoing comparisons show agreement between the numerical and graphical solutions. The major difference in the cracking boundaries from the two methods is attributed to the effects of the load acting after separation and of particle velocity on wave velocity. The points available from the numerical analysis are consistent with the graphical spall boundary, but more points are needed to establish the significance of the protrusion attributed to the effect of separation.

References

[1] Bungay, R. W., "Estimated Bounds on Suddenly Applied Loads Required to Damage the Heat Shield on a Hardened Reentry Vehicle," Semiannual Technical Summary Rept. 1, Contract AF 29(601)-6251, July 1964, Stanford Research Inst., Menlo Park, Calif.

[2] Stuiver, W., "Graphical Method for Analysis of Matched Pulses," *AIAA Journal*, Vol. 6, No. 4, April 1968, pp. 762–764.
[3] Stuiver, W., "On the Concept of Matched Pulses for Two-Layer Laminates," AIAA/ASME 8th Structures, Structural Dynamics and Materials Conference, New York, 1967.
[4] Samuelsen, G. S., Stuiver, W., and Abrahamson, G. R., "Critical Load Curves for Rebound Cracking," Final Rept., Contract AF 29(601)-6828, March 1967, Stanford Research Inst., Menlo Park, Calif.
[5] von Neumann, J. and Richtmyer, R. D., "A Method for the Numerical Calculations of Hydrodynamic Shocks," *Journal of Applied Physics*, Vol. 21, March 1950, pp. 232–237.
[6] White, M. P. and Griffis, L., "The Propagation of Plasticity in Uniaxial Compression," *Journal of Applied Mechanics*, Vol. 70, 1948, pp. 256–260.
[7] Woods, D. S., "On Longitudinal Plane Waves of Elastic-Plastic Strain in Solids," *Journal of Applied Mechanics*, Vol. 19, Dec. 1952, pp. 521–525.
[8] Morland, L. W., "The Propagation of Plane Irrotational Waves Through an Elastoplastic Medium," *Philosophical Transactions of The Royal Society (London)*, Vol. 251, June 1959, pp. 341–383.
[9] Erkman, J. O., "Artificial Viscosity Code for One-Dimensional Shock Waves," in Duvall, G. E. and Alverson, R. C., "Fundamental Research in Support of Vela-Uniform," Semi-annual Technical Summary Rept. 4, Contract AF 49(638)-1086, July 1963, Stanford Research Inst., Menlo Park, Calif., pp. 1–7.
[10] Wilkins, M. L., "Calculations of Elastic-Plastic Flow," *Methods in Computational Physics, Vol. 3, Fundamental Methods in Hydrodynamics*, Academic Press, New York, 1964, pp. 211–262.

NOVEMBER 1971 AIAA JOURNAL VOL. 9, NO. 11

Experimental Investigation of Panel Divergence at Subsonic Speeds

THORSTEINN GISLASON JR.*
Dartmouth College, Hanover, N. H.

An experimental investigation has been conducted of the post-divergence, as well as the onset of divergence, behavior of a flat, rectangular panel at low airspeeds. Comparisons with available nonlinear theory show qualitative agreement for panel strain as well as for the dynamic pressure at the onset of divergence, except for the thinnest panel tested, where experimentally measured strains were substantially higher than those predicted theoretically. It is thought that geometric imperfections were largely responsible for this difference.

Nomenclature

a = panel length
b = panel width
D = $Eh^3/12(1 - \nu^2)$, panel flexural stiffness
E = Young's modulus
h = panel thickness
K = dimensionless frequency
M = Mach number
Δp = static pressure difference across the panel
q = dynamic pressure
q_D = dynamic pressure at panel divergence
R_T = $12(1 + \nu)\alpha(a/h)^2\Delta T$, non-dimensional temperature differential
ΔT = temperature difference between panel and frame
ΔT_b = temperature difference required to buckle panel
U = air speed
w = panel displacement in z direction
x = chordwise spatial variable
y = spanwise spatial variable
α = coefficient of thermal expansion
ρ = density of air
ρ_m = density of the panel
λ^* = nondimensional dynamic pressure
$\lambda_f{}^*$ = nondimensional flutter dynamic pressure
ν = Poisson's ratio
ϵ = strain
ω = cyclic frequency

Received November 3, 1970; revision received May 12, 1971. I wish to acknowledge the helpful assistance given me by my advisor, E. H. Dowell of the Aerospace and Mechanical Sciences Department of Princeton University. Also assisting me in this work was C. S. Ventres of the Aerospace and Mechanical Sciences Department, Princeton University.

* Graduate Student.

I. Introduction

A. The Problem and Its History

FOR sufficiently thin panels static divergence can occur at a lower dynamic pressure than does flutter, usually at subsonic speeds only, and if it does occur, is in most cases a mild type of instability. Emphasis has heretofore been on high Mach number panel flutter. Panel divergence is thought to be understood mathematically, but very little work has been done on experimental panel divergence.[1]

Physically, divergence occurs when the aeroelastic system becomes statically unstable. Theoretically, the linear response of the system grows exponentially with time. In practice, the nonlinear response will reach some static equilibrium diverged condition after some exponential temporal growth. This diverged condition as well as the onset of divergence will be considered here.

One of the most active researchers in the field of panel divergence is Ishii.[2] Mention should be made of the work of Richardson and Johns,[1,3] Dugundji, Dowell, and Perkin,[4] and Sykes and Thomas.[1,3]

B. Discussion of the Important Physical Parameters

Midplane load is one of the most important parameters in divergence. Tension often prevents catastrophic failure in the presence of restrained edges because the restoring force increases nonlinearly faster than deformation. Ishii has attempted to minimize midplane load in his experiments by mounting the trailing edge of the panel without restraints, and applying a constant mid-plane force. He has been quite suc-